ISBN: 978-3-95450-222-6 ISSN: 2673-5350 doi:10.18429/JACoW-IBIC2020-TUPP10

Content from this work may be used under the terms of the CC BY 3.0 licence (© 2020). Any distribution of this work must maintain attribution to the author(s), title of the work, publisher, and DOI

X-RAY BEAM POSITION MONITOR SILICON PHOTODIODE MEASUREMENTS FOR THE ADVANCED PHOTON SOURCE UPGRADE*

K. P. Wootton†, H. P. Cease, M. J. Erdmann, S. Oprondek, M. Ramanathan, B. X. Yang
Argonne National Laboratory, Lemont, IL, USA

Abstract

To best leverage the orders of magnitude average brightness increase of multi-bend achromat synchrotron radiation storage rings, ambitious beam stability requirements are imposed. One system that will be employed at the Advanced Photon Source Upgrade in support of photon beam stability will be X-ray beam position monitors. In the present work, electrical characterisation of several types of photodiodes are evaluated for potential use in X-ray beam position monitors.

INTRODUCTION

In order to meet demanding photon beam stability requirements of the Advanced Photon Source – Upgrade (APS-U) [1], hard X-ray beam position monitors are planned [2–4]. Several geometries of x-ray beam position monitors for different insertion device beamlines are foreseen, based upon the grazing-incidence insertion device hard x-ray fluorescence BPM (GRID XBPM) detector geometry [2–11].

In the present work, electronic performance testing of silicon photodiodes for X-ray beam position monitors is presented.

PHOTODIODES TESTED

The photodiodes tested in these studies were Luna Opto-Electronics solderable silicon photodiodes. The diodes are intended to be operated either in a photoconductive ('C') or photovoltaic ('V') mode. These solderable photodiodes are compatible with operation in an ultrahigh vacuum environment. Diode types tested in the present work included:

- PDB-C612-2,
- PDB-C613-2,
- PDB-V615-2.

METHOD

We consider here electrical tests that can be performed throughout stages of detector assembly, cleaning and installation. During all measurements in the present work, the photodiode under test was positioned within a light-tight box.

Shunt Resistance

Shunt resistance is defined to be the average slope of the voltage-current V–I curve about 0 V. The accepted practice for the measurement of diodes is to measure the current across the diode at voltages of ±10 mV [12].

For measurement of shunt resistance, the DC power supply and picoammeter were connected in series with the photodiode. The current through the diode was measured using the picoammeter. The power supply was set to output either +10 mV, 0 mV or −10 mV.

The sequence of measurement was to measure at 0 mV, +10 mV, 0 mV, −10 mV. Three observations of the current at each voltage setpoint were made. It took some time for the picoammeter current measurement to reach equilibrium. During these tests it took approximately 30 s per voltage step for the current measurement to stabilise. In practice, this was the slowest measurement to make.

Two-Wire Resistance

One technique to measure resistance of the diode is to perform a two-wire resistance measurement [13]. The average forward resistance is measured with a digital multimeter (Keysight 34465A 6 1/2 digit multimeter) used as an ohmmeter. The measurement current is 500 nA [14]. Due to the nonlinear I–V curve of the photodiode, this resistance value is expected to change with the measurement current. This measurement only returns a value for the voltage with the leads connected in forward bias across the diode. For a normal diode measured in reverse bias, the multimeter returned an 'overload' response.

Each two-wire resistance measurement took less than one second to measure. Three observations were made at each setting.

Diode Test

A diode test is commonly included on multimeters [13]. It is a voltage measurement at a nominal current. In the present work, the current used was ∼1 mA.

Each diode test took less than one second to measure. Three observations were made at each setting.

Photocurrent

Photodiodes in the GRID XBPM are illuminated by X-ray fluorescence from a cerium-doped yttrium aluminium garnet (YAG) scintillator crystal. As a performance characteristic, we evaluate the uniformity of DC photocurrent produced by these photodiodes when illuminated by a green LED.

To evaluate the photocurrents of photodiodes, the photodiode was illuminated by a InGaAlP light emitting diode

* Work supported by the U.S. Department of Energy, Office of Science, Office of Basic Energy Sciences, under Contract No. DE-AC02-06CH11357.
† kwootton@anl.gov

ISBN: 978-3-95450-222-6 ISSN: 2673-5350 doi:10.18429/JACoW-IBIC2020-TUPP10

(LED) with a central emission wavelength of 571 which closely matches the central emission wavelength of 550 nm of the YAG scintillator. The diode was powered by a DC power supply with a 500 Ω resistor in series. The power supply for the LED was configured to operate in voltage-controlled mode. The voltage was set at each setpoint between 0 – 12 V, in steps of 2 V.

RESULTS

For each model of photodiode tested, histograms of the measured distribution of properties are presented.

PDB-C612-2

The measured shunt resistance of the PDB-C612-2 photodiodes is plotted in Fig. 1.

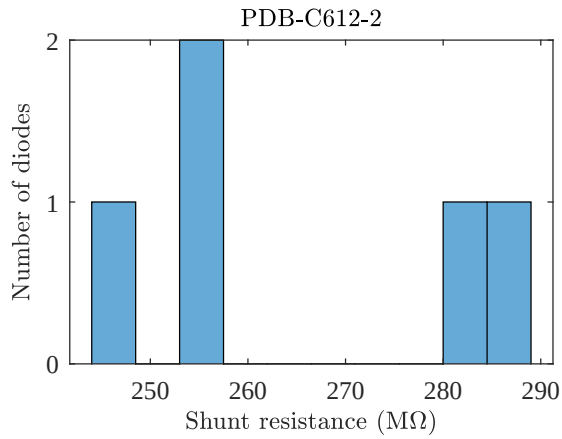

Figure 1: PDB-C612-2 shunt resistance measurements.

The measured two-wire resistance of the PDB-C612-2 photodiodes is plotted in Fig. 2.

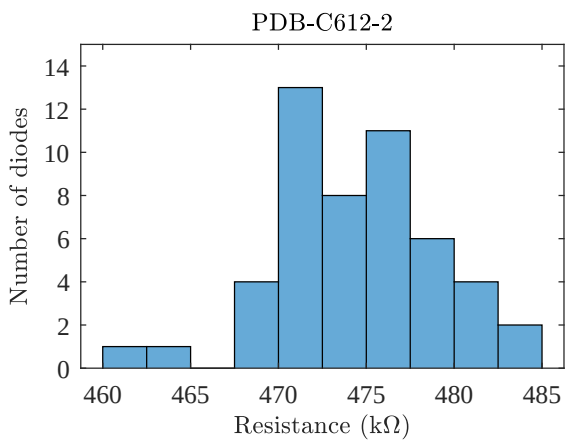

Figure 2: PDB-C612-2 two-wire resistance measurements.

The measured diode test of the PDB-C612-2 photodiodes is plotted in Fig. 3.

The photocurrent response of the PDB-C612-2 photodiodes is plotted in Fig. 4.

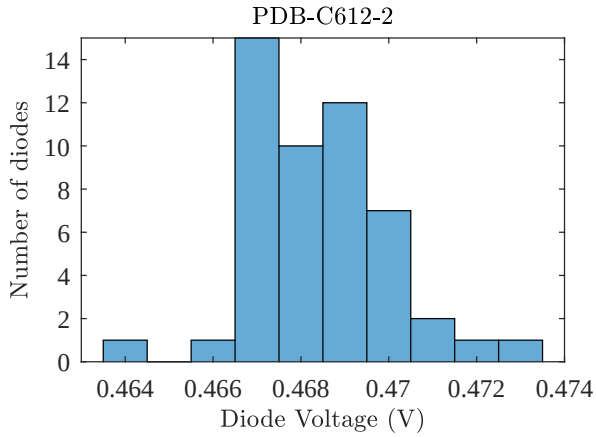

Figure 3: PDB-C612-2 diode measurements.

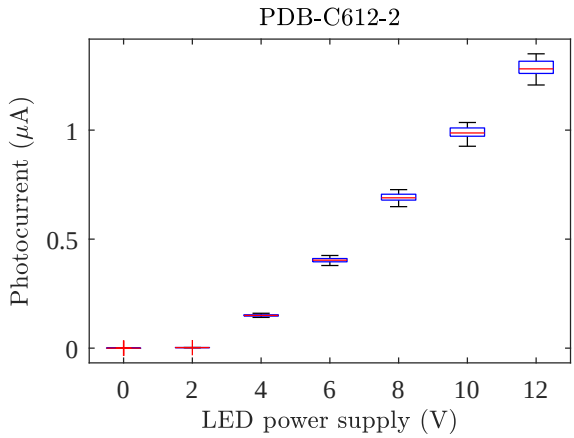

Figure 4: PDB-C612-2 photocurrent measurements.

PDB-C613-2

The measured shunt resistance of the PDB-C613-2 photodiodes is plotted in Fig. 5.

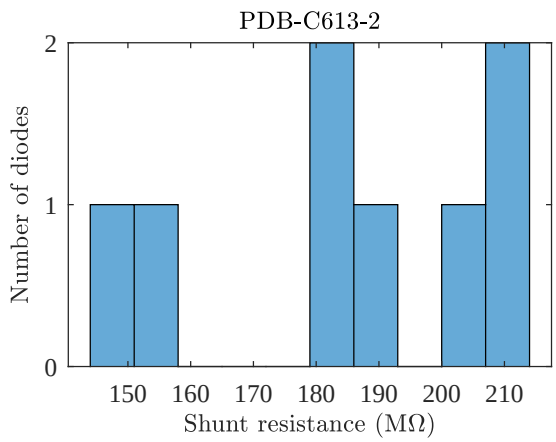

Figure 5: PDB-C613-2 shunt resistance measurements.

The measured two-wire resistance of the PDB-C613-2 photodiodes is plotted in Fig. 6.

The measured diode test of the PDB-C613-2 photodiodes is plotted in Fig. 7.

Content from this work may be used under the terms of the CC BY 3.0 licence (© 2020). Any distribution of this work must maintain attribution to the author(s), title of the work, publisher, and DOI

ISBN: 978-3-95450-222-6 ISSN: 2673-5350 doi:10.18429/JACoW-IBIC2020-TUPP10

Content from this work may be used under the terms of the CC BY 3.0 licence (© 2020). Any distribution of this work must maintain attribution to the author(s), title of the work, publisher, and DOI

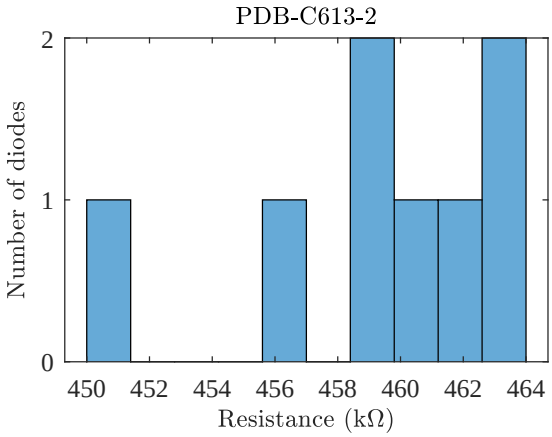

Figure 6: PDB-C613-2 two-wire resistance measurements.

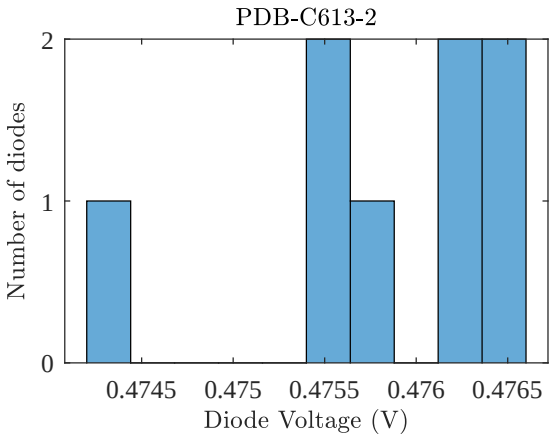

Figure 7: PDB-C613-2 diode measurements.

The photocurrent response of the PDB-C613-2 photodiodes is plotted in Fig. 8.

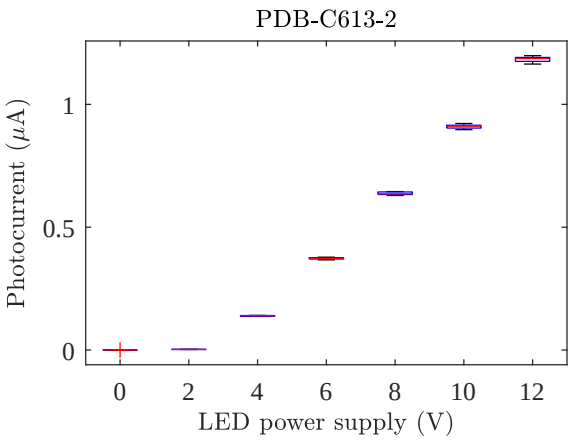

Figure 8: PDB-C613-2 photocurrent measurements.

PDB-V615-2

The measured shunt resistance of the PDB-V615-2 photodiodes is plotted in Fig. 9.

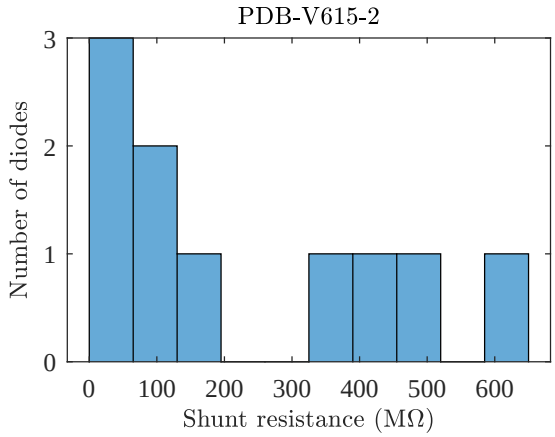

Figure 9: PDB-V615-2 shunt resistance measurements.

The measured two-wire resistance of the PDB-V615-2 photodiodes is plotted in Fig. 10.

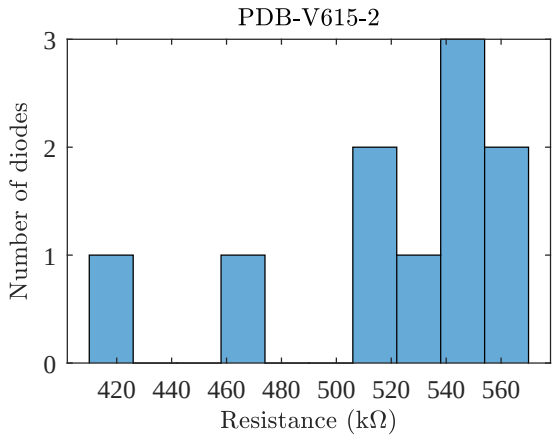

Figure 10: PDB-V615-2 two-wire resistance measurements.

The measured diode test of the PDB-V615-2 photodiodes is plotted in Fig. 11.

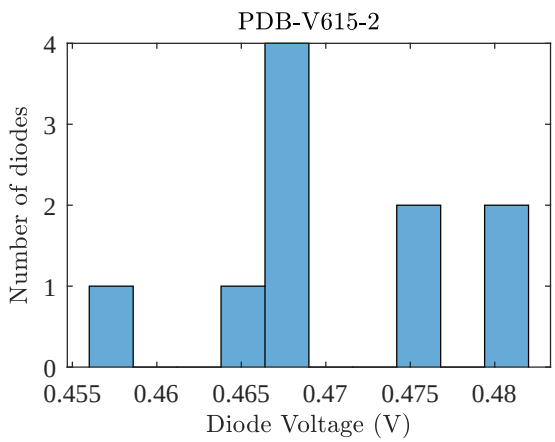

Figure 11: PDB-V615-2 diode measurements.

The photocurrent response of the PDB-V615-2 photodiodes is plotted in Fig. 12.

ISBN: 978-3-95450-222-6 ISSN: 2673-5350 doi:10.18429/JACoW-IBIC2020-TUPP10

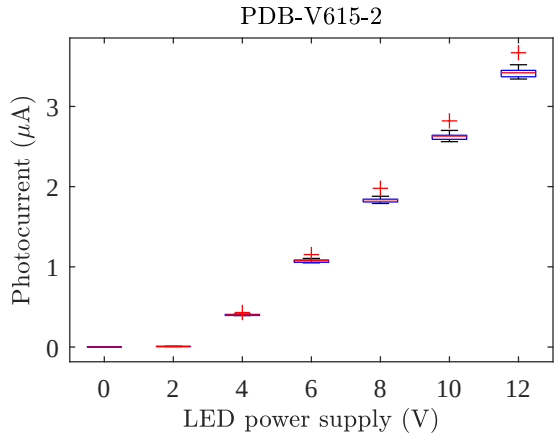

Figure 12: PDB-V615-2 photocurrent measurements.

DISCUSSION

We compared the electrical measurements of various diodes. A summary of the mean and standard deviation of these measurements is given in Table 1. The spread of photocurrent results for each type of photodiode was evaluated for the given condition of 12 V excitation of the illuminating LED.

Table 1: Mean (μ) and Standard Deviation (σ) of Batch Measurements of Photodiodes

Property	**Units**	μ_{C612}	σ_{C612}	$\frac{\sigma_{C612}}{\mu_{C612}}$ (%)
Shunt resistance	MΩ	265	19	7.1
2-wire resistance	kΩ	466	3.1	0.67
Diode voltage	V	0.465	0.001	0.28
Photocurrent	μA	1.29	0.03	2.6
Property	**Units**	μ_{C613}	σ_{C613}	$\frac{\sigma_{C613}}{\mu_{C613}}$ (%)
Shunt resistance	MΩ	186	26	14
2-wire resistance	kΩ	459	4.4	0.96
Diode voltage	V	0.476	0.001	0.16
Photocurrent	μA	1.18	0.01	0.95
Property	**Units**	μ_{V615}	σ_{V615}	$\frac{\sigma_{V615}}{\mu_{V615}}$ (%)
Shunt resistance	MΩ	220	225	100
2-wire resistance	kΩ	520	46	8.8
Diode voltage	V	0.471	0.007	1.6
Photocurrent	μA	3.44	0.10	2.8

We evaluated the statistical distribution of the diode properties using a ratio of the standard deviation over the mean (σ_i/μ_i), where i is the identifier of the photodiode model. For the PDB-V615-2 diode, the ratio (σ_i/μ_i) for the shunt resistance, two-wire resistance and diode voltage is more than an order of magnitude larger than the ratio for the PBD-C612-2 or PDB-C613-2 diodes. The statistical distribution of photocurrents appears similar for all three diode types, at about 1–3%. In future, other diode properties could additionally be measured, such as the dark current at a reverse bias of 5 V.

CONCLUSION

Electronic performance testing of silicon photodiodes for X-ray beam position monitors was presented. For the V615 diode, the statistical spread of shunt resistance, two-wire resistance and diode voltage is more than an order of magnitude larger than the ratio for the C612 or C613 diodes. The statistical distribution of photocurrents appears similar for all three diode types, within 1–3%.

ACKNOWLEDGEMENTS

The submitted manuscript has been created by UChicago Argonne, LLC, Operator of Argonne National Laboratory ("Argonne"). Argonne, a U.S. Department of Energy Office of Science Laboratory, is operated under Contract No. DE-AC02-06CH11357. The U.S. Government retains for itself, and others acting on its behalf, a paid-up nonexclusive, irrevocable worldwide license in said article to reproduce, prepare derivative works, distribute copies to the public, and perform publicly and display publicly, by or on behalf of the Government. The Department of Energy will provide public access to these results of federally sponsored research in accordance with the DOE Public Access Plan.
http://energy.gov/downloads/doe-public-access-plan

REFERENCES

[1] T. E. Fornek, "Advanced Photon Source Upgrade Project Final Design Report", Argonne National Laboratory, Lemont, IL, USA, Rep. APSU-2.01-RPT-003, May 2019. doi:10.2172/1543138

[2] G. Decker, B. X. Yang, R. M. Lill, and H. Bui, "APS Beam Stability Studies at the 100-Nanoradian Level", in *Proc. 14th Beam Instrumentation Workshop (BIW'10)*, Santa Fe, NM, USA, May 2010, paper TUCNB02, pp. 74–78.

[3] R. M. Lill, N. Sereno, and B. X. Yang, "BPM Stabiltiy Studies for the APS MBA Upgrade", in *Proc. 5th Int. Beam Instrumentation Conf. (IBIC'16)*, Barcelona, Spain, Sep. 2016, pp. 55–58. doi:10.18429/JACoW-IBIC2016-MOPG10

[4] N. S. Sereno *et al.*, "Beam Diagnostics for the APS MBA Upgrade", in *Proc. 9th Int. Particle Accelerator Conf. (IPAC'18)*, Vancouver, Canada, Apr.-May 2018, pp. 1204–1207. doi:10.18429/JACoW-IPAC2018-TUZGBD3

[5] B. X. Yang, G. Decker, P. K. Den Hartog, and S.-H. Lee, "High-Power Hard X-ray Beam Position Monitor Development at the APS", in *Proc. 14th Beam Instrumentation Workshop (BIW'10)*, Santa Fe, NM, USA, May 2010, paper TUPSM043, pp. 233–237.

[6] B. X. Yang, G. Decker, P. K. Den Hartog, S.-H. Lee, and K. W. Schlax, "Progress in the Development of a Grazing-incidence Insertion Device X-ray Beam Position Monitor", in *Proc. 24th Particle Accelerator Conf. (PAC'11)*, New York, NY, USA, Mar.-Apr. 2011, paper MOP189, pp. 441–443.

[7] B. X. Yang *et al.*, "High-Power Beam Test of the APS Grazing-Incidence Insertion Device X-ray Beam Position Monitor", in *Proc. 15th Beam Instrumentation Workshop (BIW'12)*, Newport News, VA, USA, Apr. 2012, paper WECP01, pp. 235–237.

Content from this work may be used under the terms of the CC BY 3.0 licence (© 2020). Any distribution of this work must maintain attribution to the author(s), title of the work, publisher, and DOI

ISBN: 978-3-95450-222-6 ISSN: 2673-5350 doi:10.18429/JACoW-IBIC2020-TUPP10

Content from this work may be used under the terms of the CC BY 3.0 licence (© 2020). Any distribution of this work must maintain attribution to the author(s), title of the work, publisher, and DOI

[8] B. X. Yang *et al.*, "Advanced X-ray Beam Position Monitor System Design at the APS", in *Proc. North American Particle Accelerator Conf. (NAPAC'13)*, Pasadena, CA, USA, Sep.-Oct. 2013, paper WEPSM14, pp. 1079–1081.

[9] B. X. Yang *et al.*, "Design and Development for the Next Generation X-ray Beam Position Monitor System at the APS", in *Proc. 6th Int. Particle Accelerator Conf. (IPAC'15)*, Richmond, VA, USA, May 2015, pp. 1175–1177. doi:10.18429/JACoW-IPAC2015-MOPWI014

[10] B. X. Yang *et al.*, "Performance Test of the Next Generation X-Ray Beam Position Monitor System for the APS Upgrade", in *Proc. 5th Int. Beam Instrumentation Conf. (IBIC'16)*, Barcelona, Spain, Sep. 2016, pp. 78–81. doi:10.18429/JACoW-IBIC2016-MOPG17

[11] B. X. Yang, "State of the Art X-Ray Photon BPMs for Next Generation Storage Ring Light Sources", presented at North American Particle Accelerator Conf. (NAPAC'16), Chicago, IL, USA, Oct. 2016, paper FRA1IO02, unpublished.

[12] P. C. Thompson and T. C. Larason, "Method of Measuring Shunt Resistance in Photodiodes", in *Proc. Measurement Sci. Conf. 2001*, Anaheim, CA, USA, 2001.

[13] T. R. Kupholdt, "Lessons in Electric Circuits, Volume III – Semiconductors," 5th Ed., 2009. http://www.ibiblio.org/kuphaldt/electricCircuits/

[14] *Keysight Truevolt Series Digital Multimeters Operating and Service Guide (Part Number: 34460-90901)*, Keysight Technologies, Inc., Loveland, CO, USA, Version 7, Mar. 2020, p. 166.